IOSR Journal of Humanities And Social Science (IOSR-JHSS)
Volume 26, Issue 6, Series 6 (June. 2021) 52-70
e-ISSN: 2279-0837, p-ISSN: 2279-0845.
www.iosrjournals.org

Spheroidizing in Steels: Processes, Mechanisms, Kinetic and Microstructure - A Review

Víctor Alcántara Alza[1]
[1](*Mechanics and Energy / National University of Trujillo, Perú)*

Abstract:
This article reviews the processes, mechanisms, kinetics and microstructure that are achieved with the spheroidized treatment in steels, which are intended to soften the initial structure for its subsequent conformed and machinability.
This treatment can be carried out in different ways, the most common being spheroidizing with a subcritical or intercritical annealing, in a single cycle or in several treatment cycles; but, always the transformation temperatures must be slightly below Ac1 or above. This structure is achieved by the cooperative growth of ferrite and cementite in laminar form from austenitized or by inducing a divorced eutectoid transformation, the latter achieving spheroidization by a non-cooperative movement of ferrite and cementite called the divorced eutectoid structure. Different models have been cited to explain the spheroidization mechanism, but these mechanisms explain the process, simply from the scope of lamella rupture. All of them can be applied to interpret the spheroidization mechanisms, being the model of Thermal Groove Theory the most adequate to explain the spheroidization of the deformed pearlite; but the mechanism for spheroidization of undeformed pearlite under static annealing conditions is not yet clear. The deformation itself leads to a higher degree of spheroidization, and the combination of the deformation with a suitable annealing treatment results in shorter annealing times and higher levels of spheroidization. In the spheroidizing processes of hypereutectoid steels the divorced eutectoid transformation (DET) is dominant over the pearlite reaction at lower austenitizing temperatures and slower cooling rates. The starting structures play a very important role in all spheroidizing processes.
Key Word: spheroidizingd; subritic and intercritical annealing; spheroidization mechanisms; globular cementite

---

Date of Submission: 05-06-2021 Date of Acceptance: 19-06-2021

I. Introduction

Heat treatments are one of the most used methods to improve the properties and work capacity of metal parts. By applying certain heat treatments, different properties can be achieved in the same material. One of the heat treatments applied to steel is the spheroidized treatment, which aims to soften it to improve its cold formability, as well as its machinability. This treatment is applied to both hypoeutectoid medium carbon steels and hypereutectoid steels [1].

The spheroidizing process is a heat treatment that softens the steel starting from different structures, being very common, starting from a pearlitic structure, which after a subcritical annealing close to the Ac1 point results in a mixture of spheroidized cementite surrounded by a matrix ferrite. This structure is obtained through the classic eutectoid transformation, and is widely used in hypoeutectoid medium carbon steels. On the other hand, in the case of hypereutectoid steels, it is currently common for the reaction to be of another type called: "divorced eutectoid transformation". In both cases, the driving force that produces the transformation is the reduction in interfacial energy per unit volume that exists between the two phases. The reduction in interfacial energy associated with carbide interfaces provides a powerful thermodynamic driving force for microstructural changes in steel to occur. Furthermore, the spheroidized microstructures thus obtained are the most stable that can be produced [2, 3].

The spheroidized treatment can be carried out with a subcritical or intercritical annealing in a single cycle or in several treatment cycles, but the transformation temperatures must always be slightly below Ac1 or above. If the annealing is subcritical, the treatment is of long duration at temperatures close to the critical Ac1 [4], but in this case, the process is compensated by the higher degree or percentage of spheroidization obtained [4].

The cementite phase can also be spheroidized by a quenching process and an over-tempering at a temperature close to Ac1 [5, 6]. That is, starting from a martensitic structure and applying a subsequent tempering very close to the critical temperature Ac1 with a longer time than conventional tempering (over-tempering). This occurs because many potential nucleations are ensured at the boundaries of the martensite laths as the tempering temperature increases and with rapid diffusion of carbon, resulting in the formation of a stable cementite, which is they form spheroidally way to decrease surface tension energy. These spheroidal cementite particles are generally obtained at a temperature of 700 °C close to the critical Ac1 in medium carbon steels [7]. The microstructure of steel heat treated with conventional spheroidizing has been found to show similarity to the microstructure of martensite over-tempered at high temperatures [8]. On the other hand, spheroidization is faster, starting from martensitic structures than starting from pearlitic structures, but the highest degree of spheroidization corresponds to the latter [9, 10].

The most common methods to speed up the spheroidizing process are: Heating to achieve full or partial austenitization and then holding just below Ac1, rapidly cooling above Ac1, or cycling above and below Ac1 [11, 12]; but Currently, other novel processes have been proposed to reduce the period of spheroidization heat treatment, such as the divorced eutectoid transformation in steels with high carbon content [13]; High intensity electrical pulses applied to a severely deformed eutectoid microstructure in high carbon steel wire [14]; and a repeated short-term cyclic heat treatment, keeping it at a temperature slightly higher than the Ac3 temperature, at which the austenite transformation ends during heating followed by forced air cooling [15,16]; Moreover Aluminum has been added to high carbon steels in order to retard the formation of the carbide network, which leads to high brittleness [13, 17].

O'Brien and W.F. Hosfor [18], performed spheroidization experiments on AISI 4037 medium carbon and low alloy steel; observing that in the subcritical cycle the spheroidization occurs much faster than in the intercritical cycle, so shorter times were required to achieve high formability. They found that spheroidization is faster during the subcritical process, due to the fact that a much finer pearlite is being spheroidized; instead, in the intercritical process, the opposite happens. However, the intercritical process produces larger spheroidal carbides. Subcritical spheroidization is recommended for hypoeutectoid steels, while intercritical spheroidization is necessary for hypereutectoid steels with high carbon content (> 0.80% C) to achieve spheroidization of the proeutectoid cementite [19, 20].

Regarding the spheroidization mechanisms of pearlite, the studies by YL Tian and RW Kraft [21], regarding the spheroidization of pearlite under static annealing conditions, made of two materials: AISI 1080 steel and a pure Fe-alloy. C, showed that in both cases, the initiation and development of spheroidization are associated with morphological faults such as terminations, holes and fissures in the cementite plates. In addition, during the spheroidization process, the recession of the terminations and the expansion of holes and cracks lead to the rupture of large cementite plates into small segments. In any case, the percentage of spheroidized. determined by the number of spheroids in a specific area, and the size of these spheroids play an important role in the mechanical and metallurgical properties of the finished part. The main parameters that affect the percentage of spheroidized cementite in steels are the cycle time, temperature and the initial microstructure of the steel. Thus, it should be taking in mind that whatever the cycle chosen for spheroidization, the smaller and more uniformly distributed cementite globules in the matrix result in better mechanical properties.

The objective of this article is to make a more complete review of the new spheroidized methods, their advantages and disadvantages, as well as to review the new theories about the transformation mechanisms and kinetics that explain the process, since, until the date, these mechanisms are not completely understood.

II. Spheroidized Process

Spheroidization is conventionally achieved by prolonged annealing at temperatures that depend on the type of steel and the desired mechanical properties. The process consists of transforming the biphasic pearlite structure, obtained in the eutectoid reaction, to a biphasic structure (ferrite + cementite), but with different morphology, that is, a structure formed by globules of cementite embedded in a ferrite matrix, which results in a spheroidized structure much softer than the pearlite structure before processing. Actually, the term spheroidized corresponds to the spheroidization of cementite. Spheroidization can take place by the following methods:
spheroidization of cementite. Spheroidization can take place by the following methods:

1) Long-term holding at a temperature just below Ac1 (subcritical annealing).
2) Heat to a temperature just above Ac1 and then cool very slowly in the furnace or keep it at a temperature just below Ac1 (intercritical annealing).
3) Heating and cooling alternately between temperatures that are just above and below Ac1 (cyclic anneling).

These three methods are outlined in Fig. 1. Only in the first case, the morphological transition (subcritical annealing) proceeds in the absence of any phase transformation [22].

Reports from the specialized literature infer that subcritical annealing shown in Fig. (1a) is the most efficient process for hypoeutectoid steels, while in hypereutectoid steels, the morphological change is achieved with greater security through intercritical treatment, or cyclical treatment shown in Fig.1b) and 1c) [23].

The cyclic regime shown in Fig. 1 (c) is used to accelerate the transformation of the cementite lamellas into globular form. Increasing the temperature above Ac1 facilitates dissolution of the cementite lamellas and on subsequent cooling below Ac1 the dissolution is disrupted and the lamellas break. These broken parts (which have less resistance to limit surface energy) coagulate more easily and faster. Fig. 2 shows a schematic diagram of the spheroidization of pearlite.

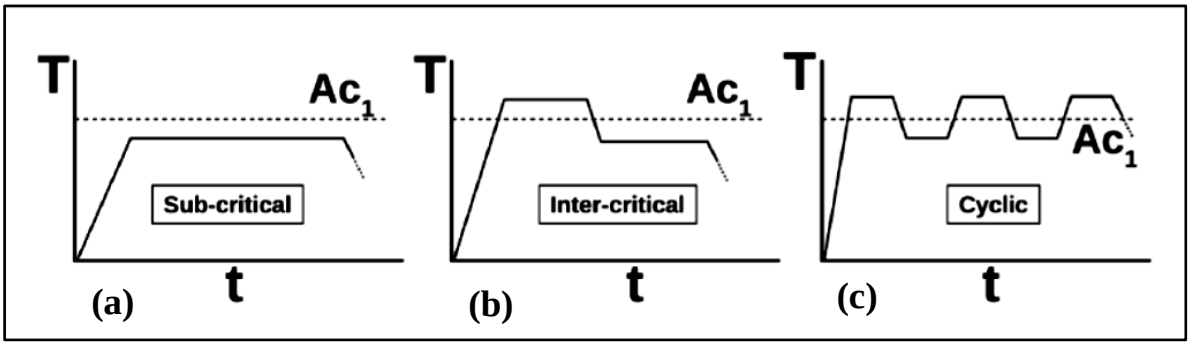

Figure 1. Typical heat treatment programs adopted to spheroidize cementite. (Ac1 represents the eutectoid temperature)

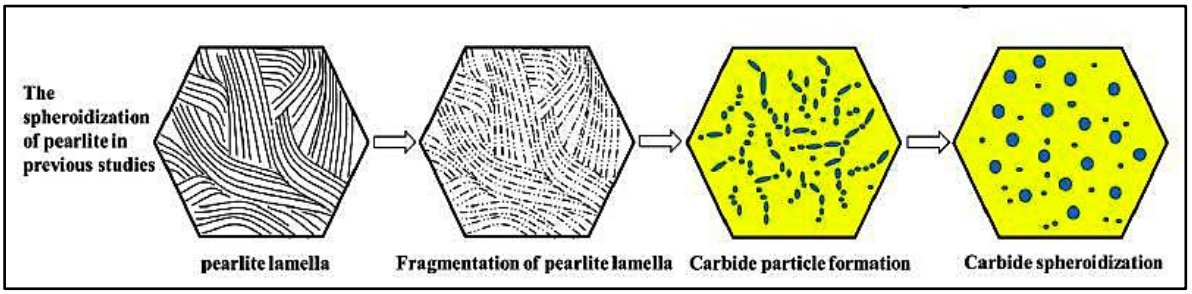

Figure 2. Schematic diagram of pearlite spheroidization

In industrial processes using any of these methods, spheroidization is achieved by keeping the steel isothermally at a temperature of 20 °C below the Ac1 point (subcritical annealing), or by heating up to 20 °C above Ac1 in which the austenite begins to form during heating, and then cooling down to 20 ° C below Ac1 and holding for a long time of hours (intercritical annealing), or by alternately heating and cooling from slightly higher to slightly lower than Ac1 temperature for 10 h or more (Cyclical annealingn) [24, 25, 26, 27]**.** However, the latter process consumes more time and energy consuming and therefore it is expensive. J. O'Brien and W. Hosford [28] reported cases of spheroidization with long times (from 12h to 20h) performed on AISI 4037 steel. They heated the steel in the intercritical temperature region (740 °C to 760 °C) ~ for 2h and then slowly cooled it below the lowest critical temperature (700 °C to 715 °C) ~ and held at this temperature for 8 to 20h and then cooled to room temperature. The microstructure obtained can be seen in Fig. 3.

In Fig. 4, the microstructures of the spheroidization of hypoeutectoid steel AISI 1040 are shown, the starting structure (Perlite + proeutectoid Ferrite) being shown in Fig. 4 (a) and after subcritical annealing at 700 °C for 24 h, a totally spheroidized structure is obtained as seen in Fig. 4(b).

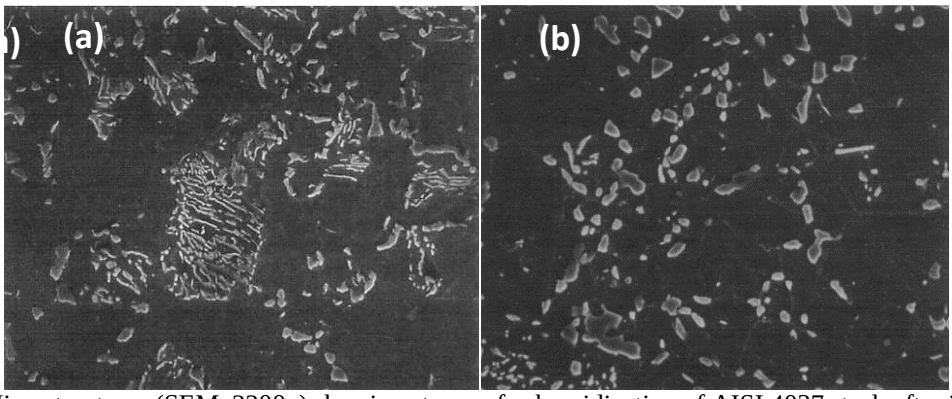

Figure 3. Microstructures (SEM, 2200x) showing stages of spheroidization of AISI 4037 steel, after intercritical annealing cycles: (a) 4 h and (b) 12 h. The spheroidization is nearly complete in (b) after 12 h. [28]

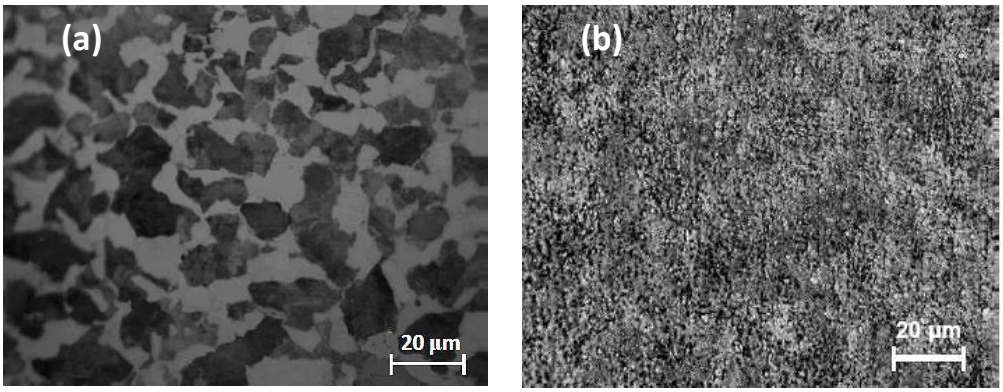

Figure 4. Spheroidized AISI 1040 steel: (a) Starting structure: (Perlite + Proeutectoid Ferrite); b) Fully spheroidized structure after subcritical annealing at 700 ° C for 24 h [29]

III. Spheroidized Hypereutectoid Steels

There are two methods for spheroidizing hypereutectoid steels. a) In the first method, the steel is annealed just below the Ac1 temperature, during which the pre-existing pearlite lamellae break into spheroids. Such a morphological transition is driven by a reduction in the total amount of the interfacial energy θ / α. (b) The second technique involves reheating the steel so that it becomes almost completely austenitic (ɣ) but with a small amount θ undissolved as spheroidal particles. On cooling through the eutectoid temperature, the pre-existing cementite particles θ that grow absorbing excess carbon that is partitioned into austenite ɣ. As the α / ɣ transform front evolves, leading to a final structure of coarse θ particles dispersed in an α-ferrite matrix. The final transformation product is known as a divorced eutectoid, since the evolutionary phases no longer grow cooperatively.

In hypereutectoid steels, the second method corresponding to intercritical spheroidization is generally applied, first heating, above the Ac1 temperature, in order to spheroidize and partially dissolve the cementite of the grain boundaries. Therefore, the final microstructure of spheroidized hypereutectoid steels generally contains a bimodal distribution of cementite particles, [30, 31] where the large particles are mainly found at the austenite grain boundaries.

It can be added that annealing above the Ac1 temperature and then below the Acm temperature achieves an incomplete dissolution of the cementite, to give rise to an austenite with fine cementite particles that normally transform into a mixture of ferrite and cementite due to two types of reactions: By the pearlitic reaction [32] or by the divorced eutectoid transformation reaction (DET) [30, 33, 34, 35] after slow cooling. The latter leads to a soft microstructure of spherical cementite particles in a ferritic matrix. The main difference between these two reactions is that during the pearlitic reaction, the structure of the product (pearlite) grows as a coupled pair of ferrite and cementite phases, while DET is not a coupled reaction and requires the presence of fine particles, but it densely distributes cementite particles in austenite. The treatment parameters define the type of reaction that occurs. Next, a more extensive explanation of the DET transformation will be given.

3.1. Divorced Eutectoid Transformation (DET)

The method is relatively new, but it is effective as long as the parameters are adequate so that the eutectoid reaction does not result in a lamellar pearlite and proeutectoid cementite structure, but rather a spheroidized cementite structure in austenite. This transformation is called: "Divorced eutectoid transformation" (DET), in which spherical (or divorced) cementite particles grow directly from the austenite phase. These particles grow along a cellular austenite / ferrite transformation front. The procedure consists of annealing at a high temperature, where only austenite and cementite exist, and then slowly cooling to allow eutectoid decomposition, but not in lamellar pearlite, but in a mixture of spheroidized cementite in austenite. In this case the proeutectoid cementite particles simply grow and absorb excess carbon as the austenite transforms into ferrite. As a consequence, the time required to generate the final spheroidal cementite structure in ferrite is drastically reduced. This transformation occurs only at temperatures immediately below Ac1 and is replaced by lamellar transformation of pearlite at slightly lower temperatures.

The key to achieving spheroidization of cementite quickly is to change the transition mode from austenite to pearlite by controlling the thermodynamics and kinetics of the phase transition, that is, the transition mode from the traditional lamellar mechanism to the divorced eutectoid transformation. (DET) [30]. The DET is a mechanism in which carbides settle around the original granular cementite and become spherical. Therefore, spherical cementite forms in two stages; the first stage is dissolution and granulation during austenitization, the second is spheroidisation and growth by DETof the supercooled austenite.

It is well established in the literature that eutectoid transformation into steels can produce a product of transformation spheroidal cementite and ferrite with a frontal transformation, as shown in Fig. 5, starting from a normalized structure.

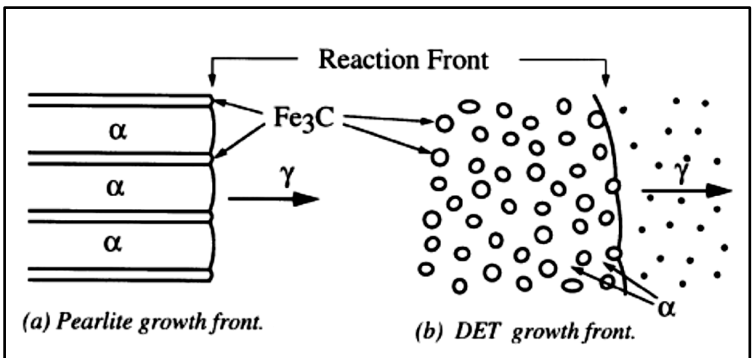

Figure 5. La geometría del frente de crecimiento para la transformación de perlita laminar en una estructura DET

H. Yang et al., [36] studied the effects of eutectoid-divorced transformation temperatures (DET) on cementite growth in GCr15 (low-alloy hypereutrctoid) bearing steel. Samples having an initial plate-shaped pearlite microstructure were used for the experimental investigation. These were heated to 780 ° C for 210 min to dissolve the granular laminar cementite and then an interrupted quenching was carried out by cooling them until reaching temperatures within a range: 750-650 ° C in which it was kept for 30 minutes and the reaction occurred. DET, achieving the respective spheroidized as shown in Fig. 6. Furthermore, it was reported DET reaction was occurred, at lower subcooling compared to the pearlitic reaction. It also the promotion of DET reaction is highly dependent on the carbide particle spacing in the austenitizing treatment.

J.D. Verhoeven and E.D. Gibson [37] has recently proposed a kinetic model for the DET reaction. This model assumes that during the transformation from austenite to ferrite, carbon diffuses from the mobile interface, in both austenite and ferrite, to the pre-existing cementite particles. Carbon diffusion fluxes cause cementite particles to grow without nucleation into new cementite particles.

It can be inferred based on the literature reviewed, that in hypereutectoid steels, the decomposition of austenite containing cementite particles can occur either by the pearlitic reaction or by the DET reaction, depending mainly on the austenitization process and the speeds of cooling. On the other hand, the DET reaction occurs at lower subcools. Compared to the pearlitic reaction, and the promotion of the DET reaction is highly dependent on the spacing of the carbide particles in the austenitizing treatment.

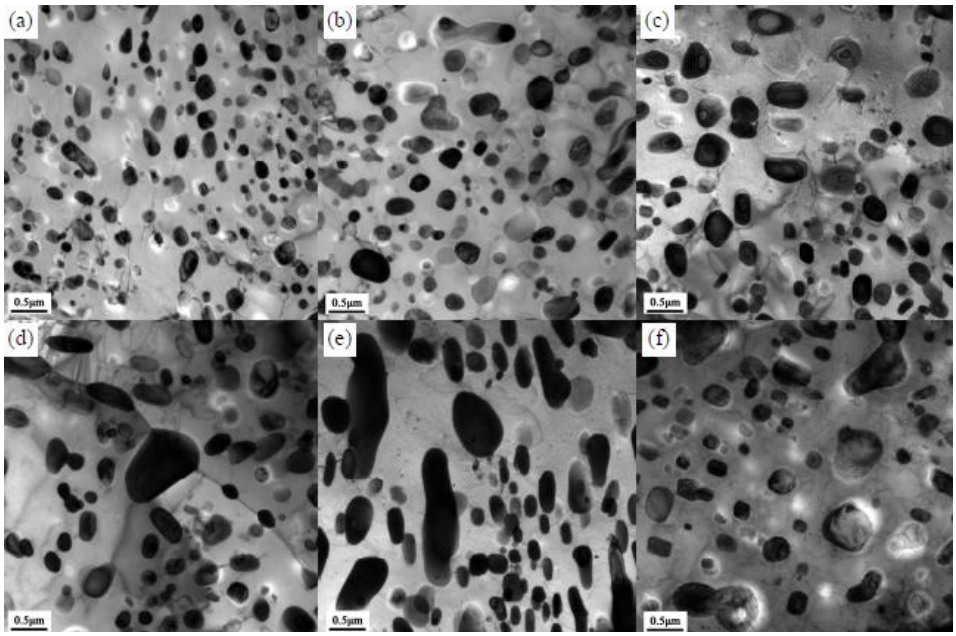

Figure 6. TEM images of investigated steel GCr15 quenched at various DET temperatures: (a) 650, (b) 680, (c) 690, (d)720, (e) 730, (f) 750°C.

IV. Influence of Deformation on the Spheroidized

Any deformation, whether cold or hot, promotes greater speed and improves spheroidization of the cementite. The greater the deformation, the greater the degree of spheroidization after annealing and thus the periods will be shorter than the conventional duration. J. Arruabarrena et al. [70] showed that when strains $e \geq 0.3$ are introduced into low-alloy, medium carbon steels, almost totally spheroidized microstructures can be obtained with a degree of spheroidization greater than 90 pct with initial microstructures of coarse or fine pearlite. Fig. 7 shows the effect of hot deformation for various strain rates applied to a low-alloy, medium carbon steel.

It should be noted that the effect of deformation-induced carbides (DIC) have a significant influence on spheroidization. Reports indicate that the effect of DIC on the spheroidization process is almost double. Carbides that precipitate at grain boundaries and strain bands are beneficial to the spheroidization process. On the other hand, the precipitation of carbide networks induced by deformation hinder the process. The existence of DIC provides nucleation sites for the newly formed carbide particles that give rise to a carbon-poor area that is transformed into ferrite. Then the ferrite matrix and spheroidized carbides will be formed directly instead of forming lamellar pearlite.

D. Hernandez-Silva et all, [38] studied the spheroidization of cementite in a medium carbon steel (AISI 1541) by subcritical and intercritical annealing. In fig. 8 shows a subcritical spheroidization process at 700 ° C starting from undeformed and deformed samples with 20% cold deformation; pre-annealed at 890 ° C. In this same reference it is reported that for this hypoeutectoid steels two important aspects must be taken into account: 1) Cold deformation prior to the process notably increases the spheroidization rate of pearlitic-ferritic microstructures 2) In undeformed specimens, the decomposition of the austenite originally formed at intercritical temperatures directly produces, in addition to new ferrite, spheroidal cementite particles. The spheroidization process in this case is even faster than wich one observed during subcritical annealing of cold worked samples.

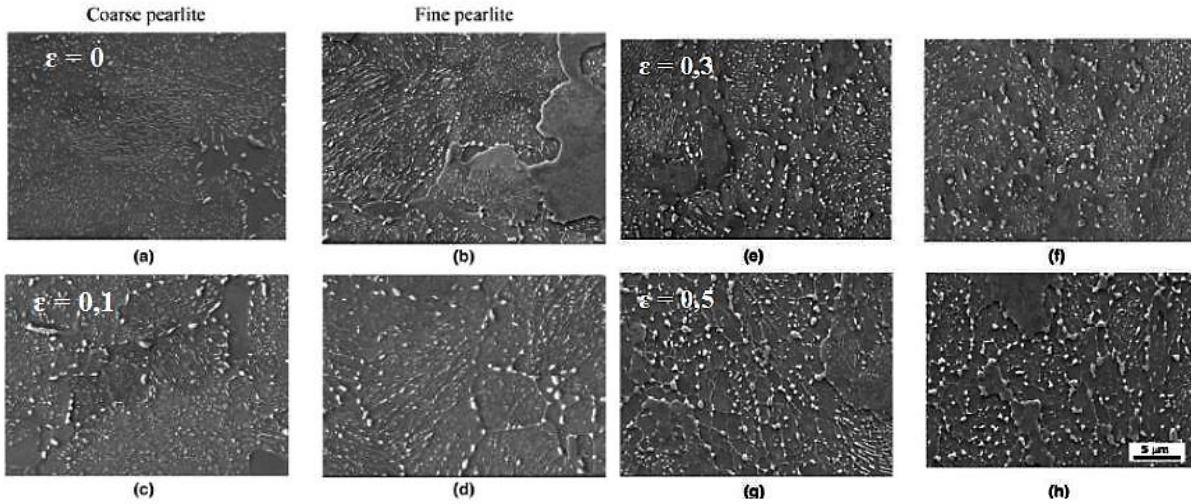

Figure 7. Microstructures developed after the application of a long spheroidization cycle [10 h (720 °C)] on (a, b) e = 0, (c, d) e = 0.1, (e, f) e = 0.3, and (g, h) e = 0.5 warm deformed coarse and fine pearlite initial microstructures.

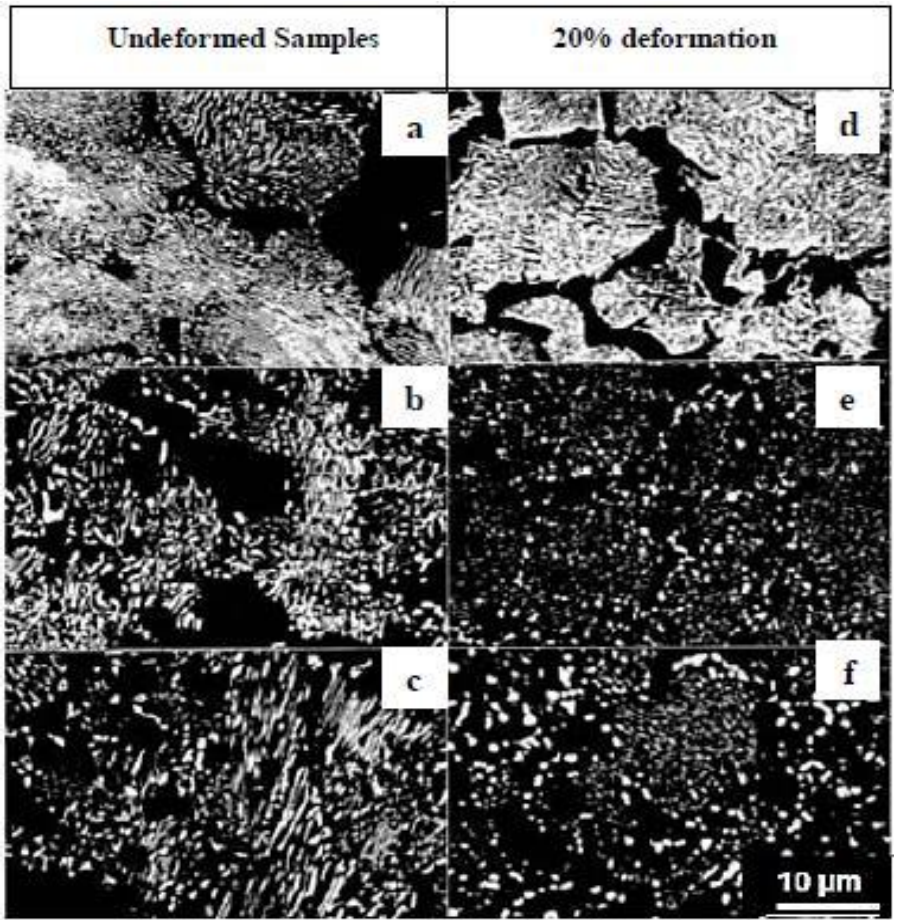

Figure 8. Microstructures pertaining to annealed samples with spheroidization treatrnent at 700 °C; a) t=0, b) t=2h, and c) t= l0h. Deformed samples (20% reduction in area) with same annealing treatment; d) t=0, e) t=2h, and f) t= l0h [38]

V. Mechanisms and Kinetics of Spheroidization

5.1. Measurement of Spheroidization Degree

Spheroidization degree is characterized by the form factor F, which was proposed by Tian and Kraft, and given by equation (1), [39]

$$F = S^c/3K_m \quad (1)$$

where S^c is the specific surface area of the cementite particles and Km is their average mean curvature. "F" can be interpreted as an aspect ratio of the particle, especially in the transformation sequence so that it starts on a platelet and goes to a spherical shape (F = 1), or vice versa; but to date, a rigorous quantitative characterization of the spherolization process is practically non-existent in the technical literature, most likely as a result of the complexity involved in the process itself [39, 40].

The actual calculation of the F values is done in terms of the quantities N_L (number of intercepts with profiles of cementite particles per unit length of the test line), V_v. (volume fraction of cementite) and N_A (profiles number of cementite particles per unit area in the observation plane), according the following equation: [39, 41]

$$F = 2N_L^2/3\pi V_v N_A \quad (2)$$

The quantitative values of N_L, Vv and N_A can be measured with the help of an image analyzer, either directly on the sample, or in SEM micrographs printed in a suitable size with a higher resolution.

5.2. Perlite Spheroidization Mechanisms

Many models have been proposed to explain the spheroidization mechanism of lamellar structures in metals; but the main three are: [42, 43]

1. Theory of capillarity induced disturbance (Rayleigh theory)
2. Theory of the thermal furrow of the grain boundary.
3. Theory of fault migration.

Although these theories are useful to explain certain aspects of the spheroidization process, there are still many aspects or phenomena that these theories cannot explain. For example, none of these models takes into account the anisotropy factor of crystallography, interfacial energy, or imperfections in microstructures. Therefore, it can be said that there is still no complete explanation of spheroidization. With this previous clarification, we will explain each one of them.

(A) Rayleigh's perturbation theory.

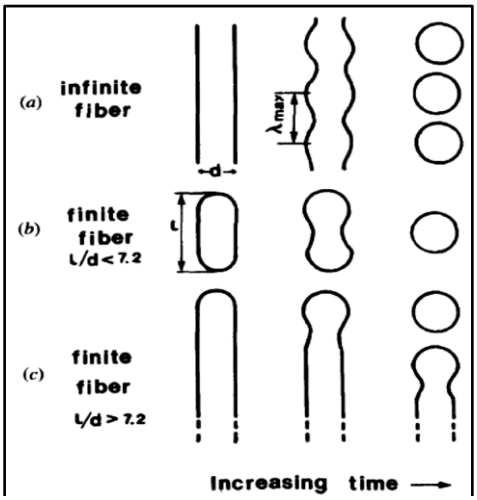

Figure. 9. Schematic representation of Rayleigh's theory for single fiber instability.

Figure 9 schematically illustrates the Rayleigh disturbance model. This model deals with the instability of a cylindrical rod caused by the disturbance induced by capillarity. It has been shown, both theoretically and experimentally [44, 45, 46, 47, 48] that a long rod shape is inherently unstable with respect to a sinusoidal disturbance as long as the wavelength of the disturbance is greater than a critical wavelength, λc. The rod would

spontaneously break into a row of spherical particles with wavelength ranges of maximum disturbance, λmax. The values of λc. and λmax depend on mass transport mechanisms.

B) Thermal Groove Theory

A model for diffusion-driven rupture of laminar structures along grain sub-boundaries is shown schematically in Fig. 10a) [43]. If a matrix of sub-limits is introduced into a laminar structure by means of deformation or phase transformation processes, an initial local equilibrium of surface tension will be obtained established at each of the triple point junctions and forms a grain boundary groove. This introduces curvature at the laminar interface and a chemical potential gradient, then it occurs diffusion of atoms that leave the curved groove in response to the chemical potential. The gradient will force the groove to grow and eventually cause a laminar plate to rupture.

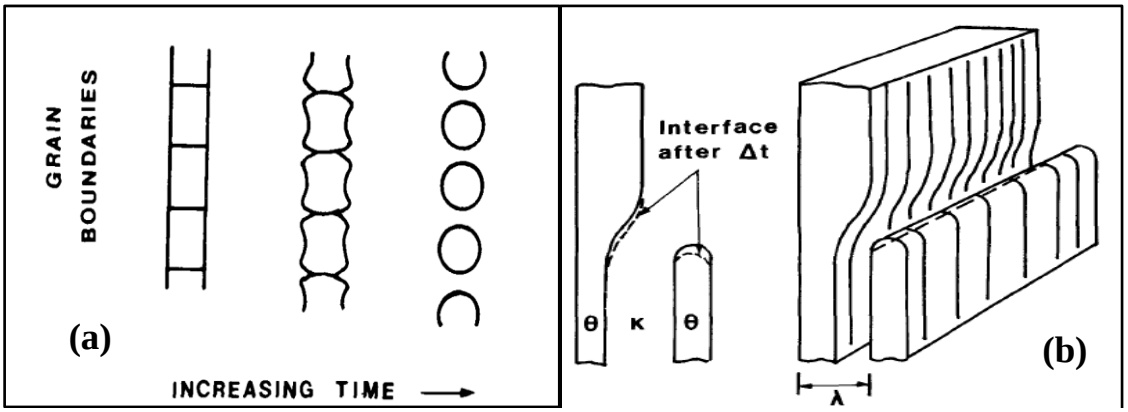

Figure 10. Schematic representation of Thermal Groove theory (a); Schematic representation of the Fault Migration Theory for the instability of lamellar structures (b)

C) Fault Migration Theory

The two previous models only deal with instabilities in isolated rods or platelets. Since the structures involved have many rods and platelets, the diffusion interactions between them must be taken into account. Two cases can be distinguished: ideal structures consisting of infinite parallel platelets or rods and real structures with finite particles and imperfections. In the first, the diffusional interaction between adjacent particles does not occur due to the absence of interfacial curvature. In the latter case, that is, in real materials, however, the interface, the curvature and therefore the chemical potential are greater in the region of the terminations than in the neighboring planar interfaces.

The driving force for spheroidization is attributed to the chemical potential gradient between a curved laminar fault and an adjacent planar interface. Atoms move from the termination to "the flat interface of neighboring plates, causing dissolution of the termination tip and thickening of the adjacent plate, as illustrated in Fig. 10b).

All these models can be applied to interpret the spheroidization mechanisms of pearlite; but, in general, it is accepted that the Thermal Groove Theory is the main mechanism for the spheroidization of the deformed perlite, since a large number of sub-limits of grain are present; But, the main mechanism for spheroidization of undeformed pearlite under static annealing conditions is not yet clear.

Finally, all of these theories are reported to have been modified as observational instruments have advanced. For example, the theory of fault migration has had to be expanded by modifying the concept of 'faults' to include all the holes, fissures and other morphological features that appear as interfaces of the high curvature in the pearlite. Such a modification is reasonable because the curved edges of these holes and cracks are substantially the same as laminar faults in terms of their physical and geometric characteristics.

5.3. Spheroidization kinetics

To describe the kinetics of the spheroidization process, the Avrami equation can be applied, in the form proposed by Nijhof [49, 50, 51]:

$$\boldsymbol{\alpha = 1 - \exp\left(-kt^{n}\right)} \tag{3}$$

Which can also be expressed as follows:

$$\alpha = [S_V (t = 0) - S_V (t)] / [S_V (t = 0) - S_V (t = \infty)] \quad (4)$$

where:
α: degree of spheroidization
S_V: parameter representing the relative area of the boundaries of the ferrite / cementite interface
S_V (t = 0): initial value of S_V corresponding to the initial state,
S_V (t): value of S_V after annealing time t,
S_V ($t = \infty$): final value of S_V; assumed: S_V = 500, mm^{-1},
k, n: equation parameters

There is no clear physical interpretation of the Avrami constants k and n. Under certain conditions, the constant k can be considered as the rate constant of the process, while the constant n can be considered as dependent on the diffusion mechanism.

5.3.1. Energía de activación (Q)

The activation energy is determined based on the Arrhenius equation:

$$k = A \times \exp((-Q) / (R \times T)) \quad (5)$$

where:
k – rate constant,
A – pre-exponentional factor,
Q – activation energy,
R – Boltzman constant,
T – temperature, K.
Para un acero al carbono eutectoide 0,76%C, se tienen los siguientes valores experimentales en la tabla 1

Table 1. Estimated activation energy of pearlite spheroidization [52].

Temperature,°C	Activation energy, *Q*	
	kJ/mol	kcal/mol
700; 680; 660; 640; 620	104.8 ±11.4	25.1 ±2.73

The speed of the spheroidization process determines the temperature; the higher the annealing temperature, the greater the progress of the process, expressing in intensity the changes of the S_V parameter over time. The parameter k in the equation. (1) can be considered as a constant rate of spheroidization process. Therefore, the activation energy Q can be determined from the temperature dependence of the constant k using the Arrhenius equation

VI. Effects of Starting Structures on Spheroidization

Different parameters such as spheroidization time and temperature and the initial microstructure of the steel affect the amount of spheroidized cementite. The spheroidization of cementite can not only be achieved starting from a laminar pearlite structure, which is the result of a eutectoid annealing; but it can also be made from other structures consisting of martensite, coarse pearlite, fine pearlite and bainite. For each case there is a different treatment cycle.

According Arai T, et al. [53]. the shortest spheroidization time and with the same time, the more evenly dispersed spheroids in the matrix are achieved from the most unstable initial microstructure (mainly martensite) of the steel being processed. The spheroidization rate in the initial unstable microstructures depends on the diffusion rate of the carbon atoms in the microstructure and their coagulation. If the initial structure is pearlite. spheroidization is produced by the coagulation of the cementite lamellae. This process can be divided into two stages. In the first, the cementite lamellae take the shape of a knuckle. As the process continues, the lamellae form globules at their ends and due the limit surface energy, these are divided into spheroids (spheroidal cementite). In the second stage, some globules of cementite (carbides) grow at the cost of finer carbide particles that later disappear. In both stages, the speed of this process is controlled by diffusion. The thicker the lamellar cementite, the more energy will be required for this process.

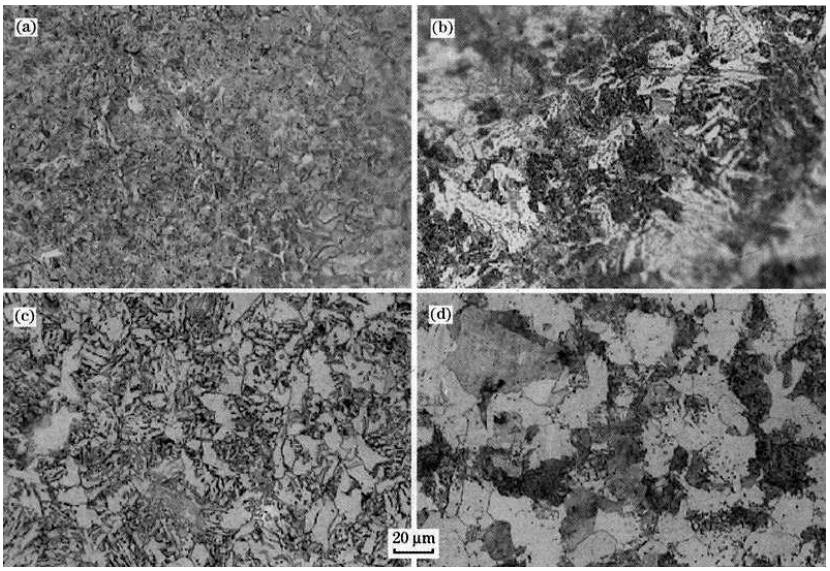

Figure 11. Starting structures of CK60 / AISI 1060 steel, before being spheroidized: (a) martensite, (b) bainite, (c) fine pearlite, (d) coarse pearlite [53]

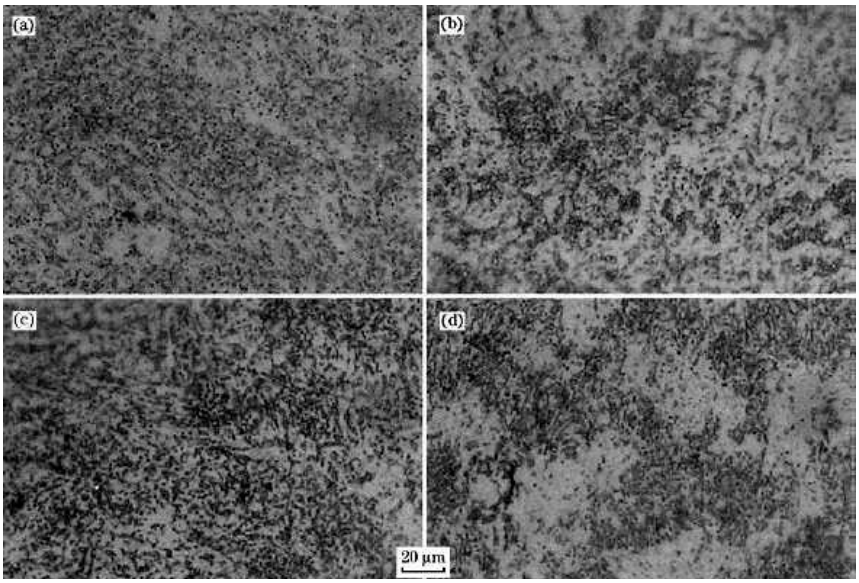

Figure 12. Spheroidal structures of CK60/AISI 1060 steel after subcritical annealing at 700 °C for 16 h [53]

Figures 11 and 12 show the results of the spheroidized processes of (CK60/AISI 1060), starting from different structures using the following parameters:

1) Martensitic microstructure: austenitized at 820 °C and then cool in water to room temperature.
2) Bainitic microstructure: austenitized at 820 °C (Cool in a salt bath at 315 °C. Keep for 90 min at 315 °C and then air cool.
3) Fine pearlitic microstructure: austenitized at 885 °C. cooling in non-turbulent air then resustenizing at 860 ° C and cooling in non-turbulent air.
4) Coarse pearlitic microstructure: austenitized at 885 °C. cooling to 700 °C. holding for 20 min at 700 ° C. and finally air cool.

Table 2 shows the percentage of spheroidization as a function of the residence time and the starting microstructure for the CK60 / AISI 1060 steel [53].

There are many reports of research work related to martensite as a starting structure itself, or as a structure prior to the route of the spheroidization process. If the starting structure is bainite, the type of bainite must be specified, due to its wide variety of morphologies that this structure presents. Thus, for example, spheroidized is not applicable in superbainite.

Hwang and De Cooman [71] investigated the effect of initial microstructure on the spheroidization of AISI 52100 bearing steel and reported that both the initial martensitic structure and the bainitic microstructure take less time to complete spheroidization than the lamellar pearlite microstructure.

I.E. Dolzhenkov and I. N. Lotsmanova [72] studied the preliminary effect of quenching (martensitic structure) on the spheroidization of carbides. Preliminary quenching was found to greatly accelerate carbide spheroidization and can be part of spheroidization treatment. For a pre-hardened steel, the austenitizing temperature and time must be selected so that a substantial percentage of the granular carbides remain undissolved. After austenitizing the previously quenching steel, the formation of lamellar carbides should be avoided, promoting a "granular pearlite" structure. Then, for the spheroidization, the cooling time and the isothermal holding temperature must be selected below Ae1.This treatment with a preliminary quenching form a new spheroidization treatment that not only shortens the spheroidization time, but also improves the properties of the parts after final heat treatment.

Table 2. Percentage of spheroidization vs spheroidization time for different starting structures of CK60/1060 steel

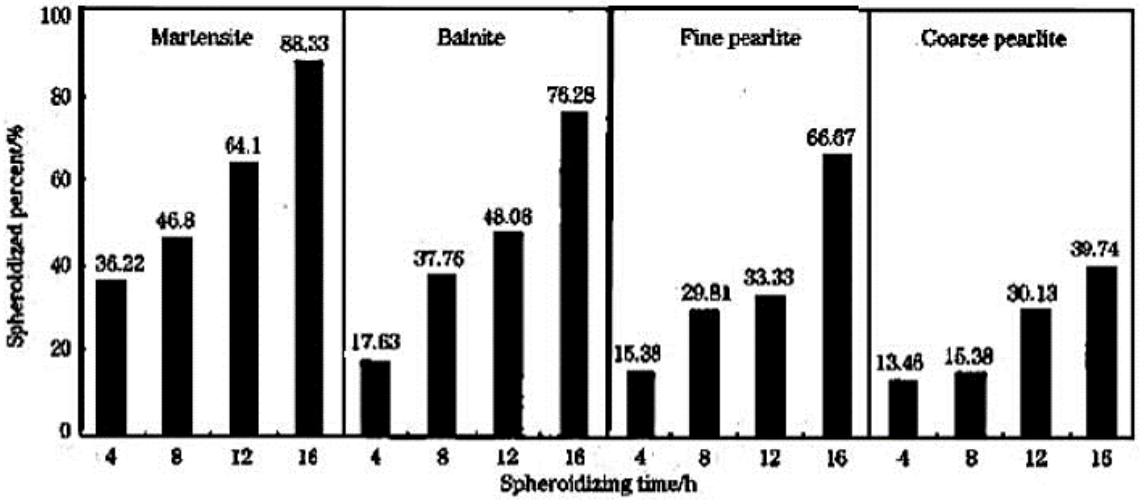

In Fig.13, the spheroidization of an AISI 1050 medium carbon steel is observed. Fig.13a) shows the starting structure (Perlite + Proeutectoid Ferrite). Fig. 13b) the spheroidized esteructure is shown applying a conventional subcritical annealing at 700°C for 12 h; incomplete spheroidization is observed. Figure 14 shows the spheroidization of a quenching sample of the same steel. Fig. 14a) shows the starting structure (Martenite Lath) obtained after austenitizing at 850 °C, for 15 min and cooled in water. Fig. 14b) shows the spheroidized structure applying a tempering at 600 °C for 1 hr. For these two cases a better result is observed starting from the laminar pearlite; although, starting from a martensitic structure, the spheroidization is not complete, with the advantage of saving time in the process [54].

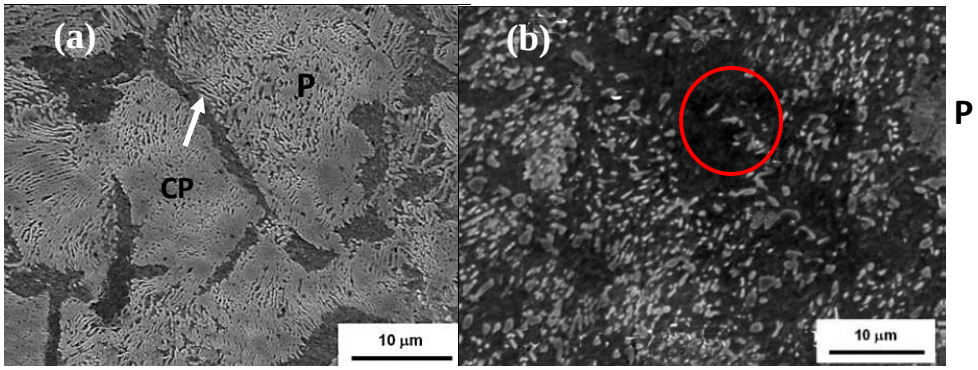

Figure 13. SEM microstructures: AISI 1050 steel: (a) Initial structure: (P + CP); (b) spheroidized structure applying a subcritical anneal at 700 ° C, 12h. [P: Perlite; CP = proeutectoid cementite]. Incomplete spheroidized, the circle indicates a non-spheroidized area. [54]

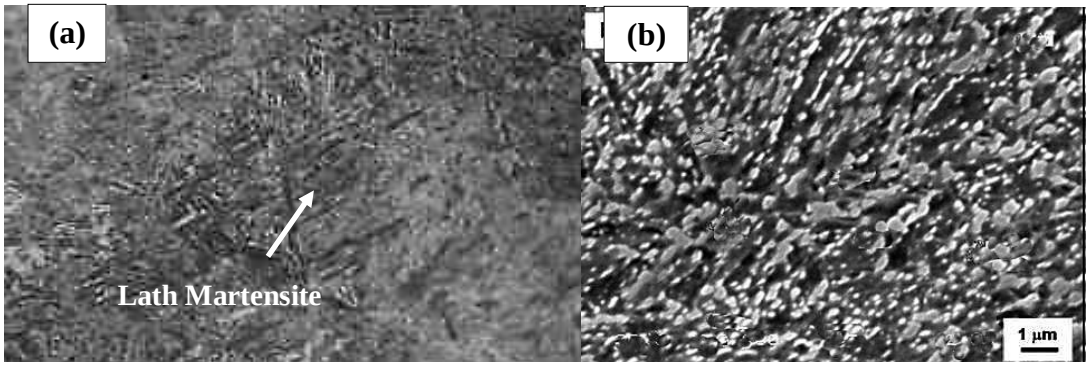

Figure 14. Microstructure of the spheroidized AISI 1050 steel: (a) starting structure: (Martensite lath); b) Spheroidized structure applying a subcritical isothermal annealing at 600 °C, for 1 h [55].

Young-Won Lee et all, [56] carried out a study on the microstructure and mechanical properties of D6AC (0.46% C) medium carbon and low alloy steel after applying a spheroidized treatment starting from martensitic samples obtained by quenching. For this purpose, two different austenitizing temperatures were adopted: 860 °C and 1000 °C with a holding time of 10 min in both cases. The samples were cooled directly in oil at room temperature to achieve a fully martensitic microstructure. Then the spheroidized treatment was applied at a temperature of 700 °C below the Ae1 temperature, and the maximum holding time was 10 h, followed by air cooling. In Fig. 15 the tempered samples that served as a starting point are observed. In Fig. 16 the resulting microstructures are shown after applying the spheroid for 1h and 4 h. In both cases, undissolved carbide particles are found in the austenitized (Cr, V and Mo carbides) that accelerate the kinetics of the spheroidized cementite particles [57]

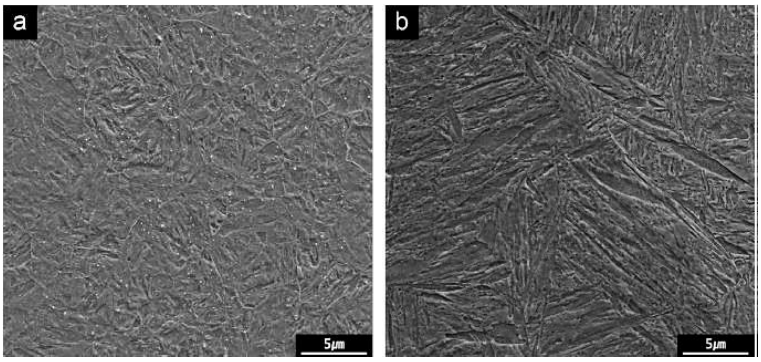

Figure 15. SEM micrographs of the as-quenched D6AC samples austenitized at (a) 860 °C and (b)1000 °C. The holding time is 10min. [56]

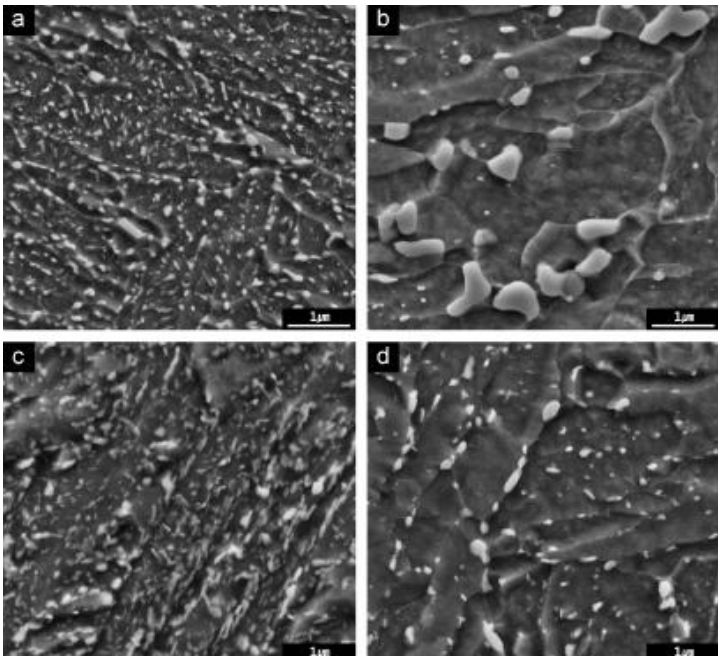

Figure 16. SEM micrographs of the spheroidized subcritico D6AC samples: (a) austenitized at 860 °C and spheroidized for 1h, (b) austenitizedat 860 °C and spheroidized for 5h, (c) austenitized at 1000 °C and spheroidized at 700°C for1h, and (d) austenitized at 1000 °C and spheroidized for 5h. The austenitizing time is 10min and the spheroidizing temperature is 700 °C. [56]

VII. Effects of Alloy Elements

The spheroidization annealing of hypereutectoid steels consists of two processes, namely: 1) intercritical austenitization and 2) subsequent slow cooling [58]. During intercritical austenitization, some cementite particles do not dissolve and are retained in austenite. After cooling, the retained cementite particles act as precipitation centers in the divorced eutectoid transformation (DET) and grow directly in the spheroidized cementite [59 - 66]. It has been widely reported in the literature that lower austenitizing temperature and slower cooling rate favor the formation of a fully spheroidized structure [59-64].

Fig. 17 shows the SEM micrographs of the steels investigated by G. Zhang [67], with different alloys after spheroidization heat treatment. For the 1C sample austenitized at 757 ° C for 30 min (Fig. 17a), the cementite particles have been completely spheroidized and show a bimodal size distribution. Some blocky cementite particles are formed at the austenite grain boundary, while smaller cementite particles are found within the austenite grains. Cementite in blocks is detrimental to the mechanical properties of high carbon steel. Compared to Fe-1C steel, the block cement particle size in 1.5Si steel (Fig. 17b) are smaller ones. For 1.5Cr steel (Fig. 17c), although the austenitizing temperature is much higher and the duration time is greater than for 1C steel, the size of the spheroidized cementite particles is much smaller; which indicates that an addition of Cr notably refines the particle size of the spheroidized cementite. However, for the 1.5 Mn steel (Fig. 3d), although the particle size of spheroidized cementite is smaller, some lamellar cementite particles are still observed.

The addition of alloying elements, in some cases promotes the spheroidization of the steels, but in others they delay it. For example, the addition of an alloying element, especially those that are strong carbide formers, such as Ti, V, Nb, and so on., which can be presented as solutes or precipitates, decrease the diffusivity of carbon in the ferrite, thus the spheroidization reaction becomes slow.

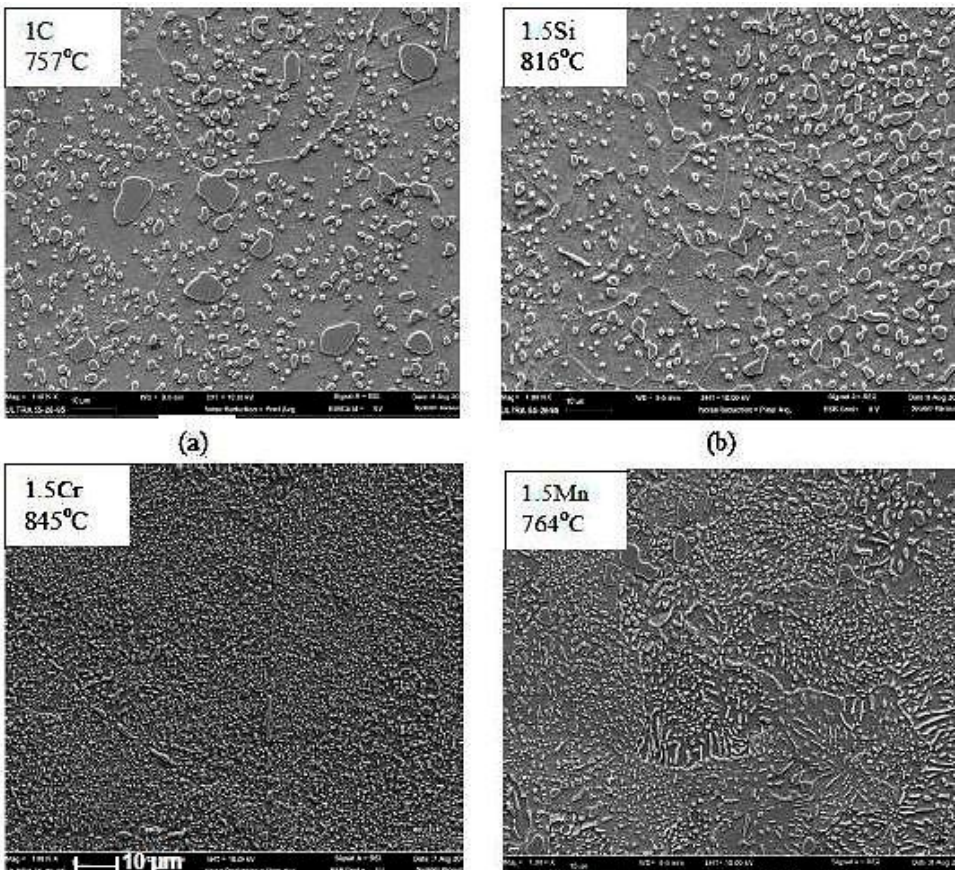

Figure 17. The typical microstucture after spheroidization annealing for (a) 1C, (b) 1.5Si, (c) 1.5Cr and (d)1.5Mn steels. The austenitizing temperatures for 1C, 1.5Si, 1.5Mn and 1.5Cr steels are 757, 816, 845 and 764 °C, respectively [67]

7.1. Aluminum Effect on Spheroidization

H.L. Yi et al. [68] studied how to accelerate the spheroidization process in eutectoid steel by adding aluminum. They established that the spheroidization process can be defined in two stages: breaking the cementite lamellae and thickening the cementite particles. Aluminum increases the spheroidization temperature by increasing the initial temperature of the austenite and thereby refines the interlaminar spacing. First, the authors establish the relationship of annealing temperature and interlaminar spacing with the two stages of spheroidization, and then explain the mechanism by which spheroidization is accelerated by the addition of aluminum. Aluminum is a strong stabilizer of ferrite and increases the eutectoid temperature during cooling and thus refines the interlaminar spacing of pearlite due to increased subcooling for eutectoid transformation, as well as suppresses lamellar growth by effect of the total diffusion of aluminum into the cementite. The refined interlaminar spacing accelerates the breakdown of the cementite flakes during the initial stage of spheroidization, but is not effective in thickening the cementite particles, which depends solely on diffusion. Furthermore, aluminum increases the initial austenite temperature during heating and thus improves the possible spheroidization annealing temperature. The elevated heat treatment temperature governs spheroidization acceleration by improving the diffusivity of the alloying elements and shows an overwhelming contribution in accelerating the thickening of cementite particles during the second stage of spheroidization.

In Fig. 18, the effect of aluminum on the spheroidization of a eutectoid carbon steel can be observed as a function of temperature and holding time, for an established percentage of aluminum [56]. In the microstructures shown, it is observed that spheroidization is more efficient when the temperature is closer to Ac1, although the treatment times are longer. Likewise, there is a great notable difference between spheroidized with aluminum (Fig 18a and 18b) and without aluminum (Fig 18c).

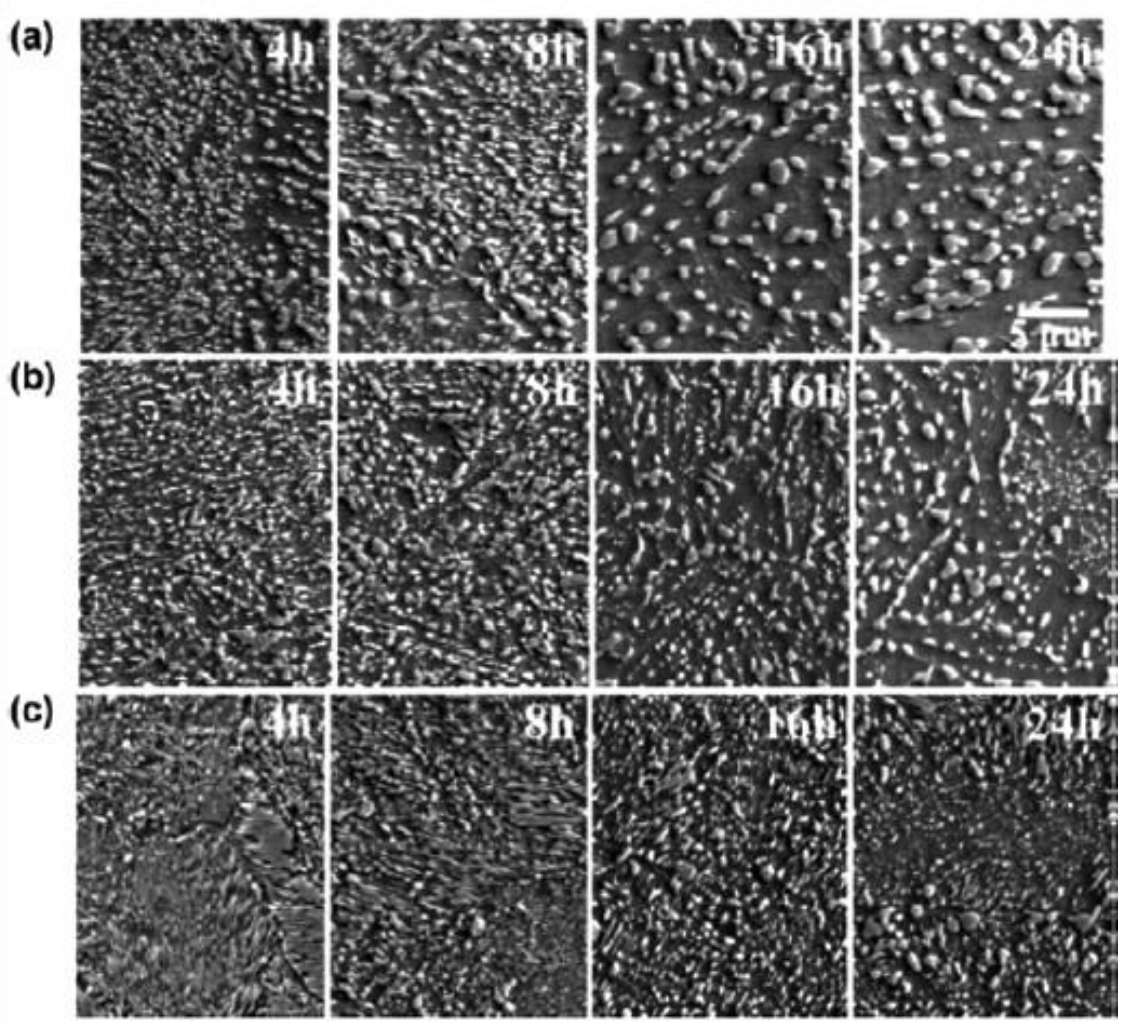

Figure 18. SEM microscopy of alloys after spheroidization for 2–24 h. (a) Alloy1 spheroidized at 700 °C; (b) alloy1 spheroidized at 650 °C (c) alloy2 spheroidized at 650 °C. (Alloy 1: with 1,93% Al; Alloy 2: without aluminum) [68]

7.2. Chromium Effect on Spheroidization

Chromium has a significant effect on the spheroidization process. The addition of chromium increases the region (temperature / time) of austenitization, so the DET reaction will occur on cooling. In steels with low content of Cr or without Cr, the promotion of the DET reaction becomes difficult. Adequate control of the spacing of the cementite particles in the austenitizing treatment and the cooling rate helps to overcome this problem and also to obtain a sufficiently spheroidized structure in steels with low Cr content.

N.V. Luzginova et al. [69] investigated the effect of Cr in the spheroidizing process of medium carbon steels. Three types of steel samples were taken: 0.5Cr; 1.5Cr and 2.5Cr. Process parameters (time and temperature) were chosen to promote TED. They found that the addition of Cr allows to obtain the spheroidized structure after austenitization at a higher temperature and a longer annealing time compared to low Cr steel, and also DET reaction takes place at low subcooling. compared to the pearlitic reaction. The microstructure obtained after the spheroidization treatment is presented in Figs. 19 (b), (c) and (d). The microstructures of the steels with 1.5Cr and 2.5Cr contents (Figures 19 (c) and (d)) show a well spheroidized structure, while the steel with 0.5Cr shows an incomplete spheroidization of the cementite (Fig. 19 (b)) where non-spheroidized areas such as the one indicated (red circle) are observed.

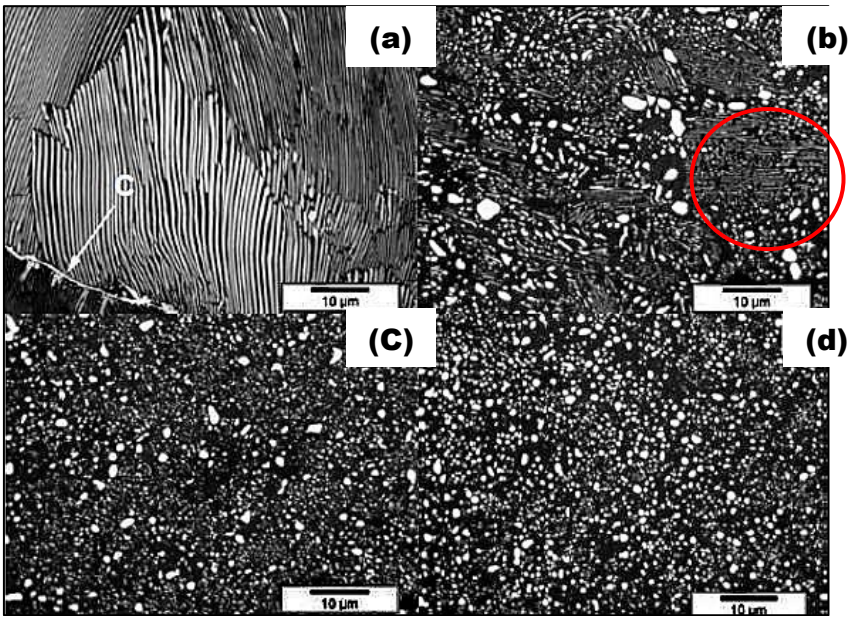

Figure 19. Microstructure 0,78 %C steel:(a) lamellar perlite without spheroidized (b), (c), (d), spheroidized structure obtained for (b) 0.5Cr, (c) 1.5Cr, (d) 2.5Cr. The presence of cementite C is observed at the grain boundaries of the structure (a).

VIII. Conclusion

After making a detailed review of the processes, mechanisms, kinetics and microstructure that are achieved with the spheroid treatment in steels, the following conclusions are drawn:

1. Cold forming and machinability of steels are improved by spheroidization treatment. The spheroidized structure consisting of cementite carbides within a ferrite matrix can be achieved in two ways: By cooperative growth of ferrite and cementite in laminar form from austensite, or by inducing a divorced eutectoid transformation DET, which achieves spheroidization in a faster way, but it has disadvantages, since it does not achieve an optimized distribution of proeutectoid cementite particles in the austenite.
2. The most widespread models have been cited to explain the perlite spheroidization mechanism, but these mechanisms explain the spheroidization process, simply from the extent of lamella rupture. This scope of spheroidization is limited since thickening of cementite particles is also involved in soft annealing treatments. Therefore, all these models can be applied to interpret the spheroidization mechanisms of pearlite. But for now, it is accepted that the Thermal Groove Theory is the main mechanism to explain the spheroidization of deformed pearlite, since a large number of grain sub-limits are presented. But the main mechanism for spheroidization of undeformed pearlite under static annealing conditions is not yet clear.
3. The initial microstructure in the spheroidization of the cementite has a significant influence on the process. In this regard, many studies have been carried out with various starting structures, but in most research works, it is observed that the microstructures have been obtained by continuous cooling from a determined austenitization temperature. But it is generally known, that in continuous cooling, the phase transformation takes place within a range of temperatures that depend on the applied cooling rate. therefore, the microstructural characteristics that are related to temperature (interlaminar spacing, thickness or length of the cementite) are not homogeneous, but different since the phase transformation begins at different moments of cooling.
4. Deformation accelerates spheroidization kinetics and leads to a higher degree of spheroidization. Various phenomena that take place during the spheroidization treatment contribute to the softening of the matrix. The combination of deformation with an annealing treatment results in shorter annealing times and higher levels of spheroidization.
5. In spheroidizing processes of hypereutectoid steels, the divorced eutectoid transformation reaction (DET) is dominant over the pearlite reaction at lower austenitizing temperatures and slower cooling rates.

References

[1]. Danyi Luo, Spheroidisation of Steel Designed for Nanostructured Bainite, Thesis to obtain the degree of Master of Philosophy in Physics (Material Science) at the University of Cambridge, 2012, London, UK.
[2]. G. Krauss, Steels Processing, Structure, and Performance, 2nd edition, Russell Township, ASM International 2015.
[3]. Z. Nasiri, H. Mirzadeh, Materwiss. Werksttech., 49 (2018) 1080-1086.
[4]. Can, A. C¸.: Material Information for Design Engineers. Istanbul, Birsen Publishing 2006.
[5]. Hoseiny, H., Klement, U., Sotskovszki, P., Andersson, J.: Materials and Design, 32, 2011, p. 21.
[6]. Podder, A. N., Bhadeshia, H. K. D. H.: Materials Science and Engineering A, 527, 2010, p. 2121.
[7]. Andres, C. G., Caruana, G., Alvarez, L. F.: Materials Science and Engineering A, 241, 1998, p. 211.
[8]. Zhang, M. X., Kelly, P. M.: Acta Materialia, 46, 1998, p. 408. doi:10.1016/S13596454(98)00046-9
[9]. E. Karadeniz, Mater. Des., 29 (2008) 251-256.
[10]. Z.Q. Lv, B. Wang, Z.H. Wang, S.H. Sun, W.T. Fu, Mater. Sci. Eng. A, 574 (2013) 143-148.
[11]. D. Hernández-Silva, R.D. Morales, J.G. Cabañas- Moreno, ISIJ Int., 32 (1992) 1297-1305
[12]. K.M. Vedula, R.W. Heckel, Metall. Trans. 1 (1970) 9-18.
[13]. B. Wang, X. Song, H. Peng, Materials and Design 28 (2) (2007) 562–568.
[14]. E. Samuel, A. Bhowmik, R. Qin, Journal of Materials Research 25 (06) (2010) 1020–1024.
[15]. A. Saha, D. Mondal, J. Maity, Materials Science and Engineering A 527 (16-17) (2010) 4001–4007.
[16]. A. Saha, D. Mondal, J. Maity, Journal of Materials Engineering and Performance 20 (1) (2011) 114–119
[17]. H. Li, B. Wang, X. Song, S. Guo, N. Gu, Journal of Iron and Steel Research, International 13(3) (2006) 9–13.
[18]. J.O´Brien, W. Hosford, Spheroidization of Medium-Carbon Steels, Journal of Materials Engineering and Performance, (1997) 6:69-72
[19]. K. Naidu and I.M. Park, Quality Annealing Economically, Wire Journal International, May 1983, p 66-70
[20]. O. Cullen, Continuous Short-Cycle Anneal for Spheroidization of Cartridge-Case Steel, Metals Progress, July 1953, p 79-82
[21]. Y. Tian,and R. Kraft, Mechanisms of Pearlite Spheroidization, Metallurgical Transactions A, Volume 18A, August 1987, 1403- 1414
[22]. J. M. O'Brien andW. F. Hosford. Spheroidization cycles for medium carbon steels. Metallurgical and Materials Transactions A: Physical Metallurgy and Materials Science, 2002.
[23]. H. K.D.H. Bhadeshia. Steels for bearings, 2012.
[24]. E. Taleff, C. Syn, D. Lesuer, O. Sherby, Metallurgical and Materials Transactions A 27 (1) (1996) 111–118.
[25]. G. TottenSteel Heat Treatment: Metallurgy and Technologies, Vol. 1, CRC Press, Boca Raton, FL, 2006.
[26]. M. Zhang, P. Kelly, Acta Materialia 46 (11) (1998) 4081– 4091.
[27]. A. Pandit, H. Bhadeshia, Proceedings of the Royal Society A: Mathematical, Physical and Engineering Science (2012).
[28]. J.M. O'Brien and W.F. Hosford, Spheroidization of Medium-Carbon Steels, JMEPEG (1997) 6:69-72
[29]. V. Alcántara, Spheroidized Heat Treatment and its Effect on Machinability in Medium Carbon Steels IOSR Journal of Mechanical and Civil Engineering (IOSR-JMCE), Volume 18, Issue 2 Ser. IV (Mar. – Apr. 2021), PP 01-13
[30]. J.D. Verhoeven: Metall. Mater. Trans. A, 2000, vol. 31A, pp. 2431–2438.
[31]. E.L. Brown and G. Krauss: Metall. Trans. A, 1986, vol. 17A, pp. 31–36.
[32]. R.F. Mehl and W.C. Hagel: Prog. Met. Phys., 1956, vol. 6, pp. 74– 134.
[33]. E.B. Damm and M.J. Merwin: in Austenite Formation and Decomposition, G.M. Michal and M.D. Novak, eds., TMS, Warrendale, PA, 2003, pp. 397–413.
[34]. W. Hewitt: Heat Treat. Met., 1982, vol. 3, pp. 56–62.
[35]. T. Oyama, O.D. Sherby, J. Wadsworth, and B. Walser: Scripta Metall., 1984, vol. 18, pp. 799–804.
[36]. H. Yang, F. Zhu, X. Liu and K. Wang, Effect of Divorced Eutectoid Transformation Temperature on Behavior of Cementite Growth in GCr15 Steel, Advanced Materials Research Vols. 194-196 (2011) pp 296-300
[37]. J.D. Verhoeven and E.D. Gibson: Metall. Mater. Trans. A, 1998, vol. 29A, pp. 1181–89.
[38]. D. Hernandez-Silva., D. Morales, J. G. Cabañas- Moreno, The Spheroidizatiom of Cementite in a Medium carbon steels by means of subcritical and Intercritical Annealing
[39]. Y. L. Tian and R. W. Kraft: Metals. Trans. A, 18 (1987), 1359.
[40]. Y Kanetsuki, M. Katsumata and H. Sawada: Tetsuo-to-Hagané. 75 (1989), 1178.
[41]. H. F. Fischmeister: Z Me!allkde., 65 (1974). 558
[42]. J.W. Martin and R. D. Doherty: Stability of Mwrostructure in Metalhc Systems, Cambridge University Press, 1976, pp. 212-16.

[43]. M. McLean: MetalScience, 1978, vol. 12, pp. 113-21
[44]. Lord Rayleigh: London Math. Soc. Proc., 1878, vol. 10, p. 4.
[45]. E A. Nichols and W. W Mullins. Trans. AIME, 1965, vol. 233, pp. 1840-48.
[46]. H.E. Cline: Acta Metall., 1971, vol. 19, pp. 481-90.
[47]. T.F. Marinis: Ph.D. Dissertation, Carnegie Mellon University, Pittsburgh, PA, 1981.
[48]. R. E Sekerka and T.F. Marinis: Proc. Int. Conf. Sohd-Solid Phase Transformations, 1981, pp. 67-84.
[49]. G.H. Nijhof, Accelerated Spheroidization of Cold Rolled Eutektoid Steel, Ph.D. Dissertation, Delftse Universitaire Pers, (1981).
[50]. G.H. Nijhof, Härterei Techn. Mitt. **35,** 59 (1980).
[51]. G.H. Nijhof, Härterei Techn. Mitt. **36**, 242 (1981).
[52]. P. Matusiewicz, J. Augustyn-Nadzieja, A.Czarski, T. Skowronek, Kinetics of Pearlite Spheroidization, Arch. Metall. Mater. 62 (2017), 1, 231-234
[53]. Arai T, Baker G M, Bates C E, et al. ASM Handbook Volume 4-Heat Treating [M]. Materials Park: ASM International, 1991.
[54]. S¸ Baday, H. Ba¸sak, A. Gural, Analysis of spheroidized AISI 1050 steel in terms of cutting forces and surface quality, Kovove Mater. 54 2016 315–320
[55]. S¸ Baday, H. Ba¸sak, A. Gural, Analysis of spheroidized AISI 1050 steel in terms of cutting forces and surface quality, Kovove Mater. 54 2016 315–320
[56]. Young-Won Lee , Young- Il Son, Seok-Jae Lee, Microstructure and mechanical properties of spheroidized D6AC steel, Materials Science & Engineering A, 585(2013)94-99.
[57]. K.G. Ata, S.A. Meisam, J. Iron Steel Res.Int.17(2010) 45–52.
[58]. H.K.D.H. Bhadeshia. Steels for bearings. Prog. Mater. Sci. 57(2012)268-435.
[59]. J. D. Verhoeven. The role of the divorced eutectoid transformation in the spheroidization of 52100 Steel, Metall. Mater. Trans. A, 31A(2000)2431-2438.
[60]. J. D. Verhoeven and E.D. Gibson. The divorced eutectoid transformation in steel. Metall. Mater.Trans. A 29A(1998)1181-1189.
[61]. K. M. Vedula and R. W. Heckel, Spheroidization of binary Fe-C alloys over a range of temperatures. Metall. Trans. 1(1970)9-18.
[62]. N. V. Luzginova, L. Zhao and J. Sietsma. The cementite spheroidization process in high-carbon steels with different chromium contents. Metall. Mater. Trans A 39A(2008)513-521
[63]. A. S. Pandit and H. K. D. H. Bhadeshia. Divorced pearlite in steels. Proc. R. Soc. A, 468(2012)2145 2767-2778.
[64]. T. Nakano, H. Kawatani and S. Kinoshita: Effects of Chromium, Molybdenum and Vanadium on spheroidization of carbide in 0.8%C steel, Trans. ISIJ, 17(1977)110-115.
[65]. Kwan-Ho Kim, Jae-Seung Lee, and Duk-Lak Lee. Effect of silicon on the spheroidization of cementite in hypereutectoid high carbon chromium bearing steels. Met. Mater. Int. 16(2010)871-876.
[66]. J. M. Beswick. The effect of chromium in high carbon bearing steels. Metall. Mater. Tran. A, 18A(1987)1897-1906.
[67]. Guohong Zhang, Dong-Woo Suh and Kaiming Wu, Effects of Mn, Si and Cr addition on the spheroidization of cementite in hypereutectoid Fe-1mass% C steel
[68]. H.L. Yi. Z.Y. Hou, Y.B. Xu, D. Wu and G.D. Wang, Acceleration of spheroidization in eutectoid steels by the addition of aluminum, Scripta Materialia 67 (2012) 645–648
[69]. N.V. Luzginova, L. Zhao, and J. Sietsma, The Cementite Spheroidization Process in High-Carbon Steels with Different Chromium Contents, Metallurgical and Materials Transactions A, Volume 39A, March 2008—513
[70]. J. Arruabarrena, B. Lopez, and J. M. Rodriguez-Ibabe., Influence of Prior Warm Deformation on Cementite Spheroidization Process in a Low-Alloy Medium Carbon Steel, Metallurgical and Materials Transactions A, 1470—Volume 45A, March 2014
[71]. H. Hwang and B.C. De Cooman: Steel Res. Int., 2016, vol. 87, pp. 112–25.
[72]. E. Dolzhenkov and I. N. Lotsmanova, Effect of Preliminary Quenching on Spheroidization of Carbides, Dnepropetrovsk Metallurgical Institute. Translated from Metatlovedenie i Termicheskaya Obrabotka, Metallov, No. 3, pp. 27-31, March, 1975.

Víctor Alcántara Alza. "Spheroidizing in Steels: Processes, Mechanisms, Kinetic and Microstructure - A Review."*IOSR Journal of Humanities and Social Science (IOSR-JHSS)*, 26(06), 2021, pp. 52-70.